Downregulation of complement factor H attenuates the stemness of MDA-MB-231 breast cancer cells via modulation of the ERK and p38 signaling pathways

SOON YONG PARK*, DA-YOUNG EUM*, YUNHO JIN, CHAE YOUNG LEE, JAE WOONG SHIM, SI HO CHOI, SEONG-JOON PARK, KYU HEO and YOO JIN CHOI

Research Department of Oncology, Dongnam Institute of Radiological & Medical Sciences, Busan 460333, Republic of Korea

Received May 26, 2023; Accepted September 15, 2023

DOI: 10.3892/ol.2023.14107

Abstract. The complement system is a powerful innate immune system deployed in the immediate response to pathogens and cancer cells. Complement factor H (CFH), one of the regulators involved in the complement cascade, can interrupt the death of target cells. Certain types of cancer, such as breast cancer, can adopt an aggressive phenotype, such as breast cancer stem cells (BCSCs), through enhancement of the defense system against complement attack by amplifying various complement regulators. However, little is known about the association between CFH and BCSCs. In the present study, the roles of CFH in the CSC characteristics and radioresistance of MDA-MB-231 human breast cancer cells were investigated. CFH knockdown in MDA-MB-231 cells decreased the viability of the cells upon complement cascade activation. Notably, CFH knockdown also decreased cell survival and suppressed mammosphere formation, cell migration and cell invasion by attenuating radioresistance. Additionally, CFH knockdown further enhanced irradiation-induced apoptosis through G2/M cell cycle arrest. It was also discovered that CFH knockdown attenuated the aggressive phenotypes of cancer cells by regulating CSC-associated gene expression. Finally, by microarray analysis, it was found that the expression of erythrocyte membrane protein band 4.1-like 3 (EPB41L3) was markedly increased following CFH knockdown. EPB41L3 inhibited ERK and activated the p38 MAPK signaling pathway. Taken together, these results indicated that CFH knockdown attenuated CSC properties and radioresistance in human breast cancer cells via controlling MAPK signaling and through upregulation of the tumor suppressor, EPB41L3.

Correspondence to: Dr Yoo Jin Choi, Research Department of Oncology, Dongnam Institute of Radiological & Medical Sciences, 40 Jwadong-gil, Gijang, Busan 460333, Republic of Korea
E-mail: cyj5325@dirams.re.kr

*Contributed equally

Abbreviations: BCSCs, breast cancer stem cells; CFH, complement factor H; CRPs, complement regulatory proteins; CXCR4, C-X-C motif chemokine receptor 4; EPB41L3, erythrocyte membrane protein band 4.1-like 3; NHS, normal human serum; TNBC, triple-negative breast cancer

Key words: CFH, radioresistance, cancer stemness, TNBC, MAPK pathway

Introduction

Breast cancer is one of the most common types of cancer in women worldwide. Over the last few decades, various advanced diagnostic methods and treatments, such as novel drugs and targeted therapies, have been developed; however, patients are still subject to physical and mental stress (1). Additionally, recurrence and metastasis remain critical causes of poor prognosis in patients with breast cancer (2). According to reported studies, breast cancer stem cells (BCSCs) are closely linked to these problems as BCSCs can trigger tumor progression, recurrence and metastasis through their specific characteristics, including the ability to escape immune surveillance and resistance to drugs and radiation (3-6). Additionally, BCSCs possess characteristic stem cell abilities, such as self-renewal and differentiation into heterogeneous common cancer cells (7). The $CD24^{-}/CD44^{+}$ population, a representative CSC phenotype in human breast cancer cells, exhibits enhanced survival, proliferation, clonogenicity, drug efflux, migration and invasion capacities (8,9). This population also exhibits gene expression patterns that differ from those of common cells, not only stemness-associated genes, such as Oct4, Sox2, c-Myc and Klf transcription factor 4, but also typical CSC-associated genes are upregulated (10-13). Hence, the need to find new BCSC targets is urgent to maximize the potential of current therapies.

The complement cascade is a multifunctional innate immune mechanism that provides an effective defense system against pathogens (14). This system can be activated by three pathways: The classical, mannose-binding lectin and alternative pathways (15). Various components produced in the complement activation process, such as C3a, C5a and C3b, can interact with other immune cells. C3a and C5a, known as anaphylatoxins, stimulate the inflammatory response by recruiting neutrophils and monocytes (14). Additionally, C3b

and C4b can inactivate toxic particles by binding the pathogen membrane and opsonizing pathogens for phagocytosis by macrophages (16). By contrast, complement regulatory proteins (CRPs) can prevent the activation of immune cells and the death of pathogens. Among CRPs, complement factor H (CFH) acts as a major regulator of this process through its inhibitory effects on multiple steps, including the production of C3Bb, C3b and C3bB (17,18). CFH is mostly expressed in healthy liver cells but is also upregulated in several types of cancer cells, including liver, lung, ovarian and breast cancer cells (19-23). CFH is mainly present in the extracellular space and blood, due to its secretion from cells, and the cytoplasm and cytoplasmic membrane. According to previous studies, CFH enhances cancer progression and tumorigenesis by binding C3 in the cytoplasm of lung cancer cells, and downregulation of CHF in lung cancer cells suppresses tumor growth. (20,21) CFH also regulates the stemness of liver cancer cells via late SV40 factor (19). Notably, breast cancer cells exhibit resistance to complement-mediated lysis based on their high expression levels of the CRPs, CD55 and CD59 (24). However, little is known about the direct association between breast cancer cells and CFH. Therefore, the present study aimed to elucidate the impact of CFH downregulation on radioresistance and cancer stemness in MDA-MB-231 human breast cancer cells.

Materials and methods

Survival analysis. The Cancer Target Gene Screening database (http://ctgs.biohackers.net) was used to analyze the significance between the survival period of patients with breast cancer and gene expression levels [dataset: Molecular Taxonomy of Breast Cancer Consortium (METABRIC), http://ctgs.biohackers.net/datasets/]. All primary data were deposited at The European Genome-phenome-Archive (EGA; accession no. EGAS00001001753) and were published by Pereira *et al* (25) in 2016. Data from the METABRIC dataset, including information for 1,980 patients with breast cancer, were analyzed. High and low gene expression was determined by the median. $P<0.05$ was considered to indicate a statistically significant difference. The survival and survminer packages in R (version 4.2; http://www.r-project.org/) were used for conducting survival analysis, which was validated using the Cox proportional hazards model.

Cell culture. MDA-MB-231 (human breast adenocarcinoma cell line) and Hs578T (human breast carcinoma cell line) cells were maintained in Dulbecco's Modified Eagle's Medium (DMEM; cat. no. 010-013-CV; Corning, Inc.) supplemented with 10% fetal bovine serum (FBS; cat. no. 35-015-CV; Corning, Inc.) and 1% Antibiotic-Antimycotic (cat. no. 15240-062; Gibco; Thermo Fisher Scientific, Inc.) at 37˚C in a humidified incubator with 5% CO_2. T47D, ZR751 and BT549 cells (human breast carcinoma cell lines) were maintained in RPMI-1640 medium (cat. no. 10-040-CV; Corning, Inc.) supplemented with 10% FBS and 1% Antibiotic-Antimycotic at 37˚C in a humidified incubator with 5% CO_2. MCF7 cells (human breast adenocarcinoma cell line) were maintained in Minimum Essential Medium Eagle (LM007-54; Welgene, Inc.) supplemented with 0.01 mg/ml human insulin (cat. no. I9278; MilliporeSigma; Merck KGaA), 10% FBS and 1% Antibiotic-Antimycotic at 37˚C in a humidified incubator with 5% CO_2.

Reverse transcription-quantitative PCR (RT-qPCR). RNA was isolated from cells using a Ribospin RNA purification kit (cat. no. 304-150; GeneAll Biotechnology Co., Ltd.), and cDNA was synthesized using a Thermal Cycler Dice PCR machine (Takara Bio, Inc.) with PrimeScript™ RT Master Mix (cat. no. RR036A; Takara Bio, Inc.), according to the manufacturer's instructions. qPCR was performed using a CFX96 Optical Reaction module (Bio-Rad Laboratories, Inc.) with TB Green Premix (cat. no. RR420A; Takara Bio, Inc.) according to the manufacturer's instructions. Quantification was performed by calculating the ΔCq value of the target gene relative to the Cq value of b-actin, used as a loading control (26). Information regarding the primers used for the RT-qPCR is provided in Table SI.

Short hairpin (sh)RNA knockdown. The vector used for shRNA knockdown was based on pLKO.1 and utilized the second-generation system. 293T cells were transfected with a mixture containing non-silencing (NS; negative control) or CFH-targeting shRNA (6.5 μg), viral packaging DNA (5 μg of psPAX2 and 2 μg of pMD2G) and 30 μl of X-tremeGENE 9 DNA Transfection Reagent (cat. no. 06-365-809-001; Roche Diagnostics) in 500 μl of Opti-MEM (#31985-070, Gibco), for 48 h at 37˚C in a humidified incubator with 5% CO_2. The resulting supernatant was filtered using a 0.45-μm syringe and mixed with DMEM (2 ml supernatant and 8 ml DMEM) and Polybrene infection/transfection reagent (cat. no. TR-1003-G; MilliporeSigma; Merck KGaA). Next, MDA-MB-231 cells were infected with the viral mixture for 24 h at 37˚C in a humidified incubator with 5% CO_2. The infected cells were washed with 1X DPBS and maintained in complete DMEM. After 48 h, the infected cells were incubated with selection medium containing 1 μg puromycin in 10 ml complete DMEM for 72 h at 37˚C in a humidified incubator with 5% CO_2. The cells were cultured in complete DMEM with a concentration of 0.5 μg/ml puromycin for maintenance after selection. Information regarding the shRNA used for CFH knockdown is provided in Table SII.

Western blotting. Proteins were extracted from cells using ProEX™ CETi lysis buffer (cat. no. TLP-121CETi; TransLab) and quantified using Protein Assay Dye Reagent Concentrate (cat. no. 5000006; Bio-Rad Laboratories, Inc.). Quantified proteins (20 μg) were mixed with 4X sample buffer (cat. no. B0007; Thermo Fisher Scientific, Inc.) and loaded on Bolt™ 4-12% Bis-Tris precast gels (cat. nos. NW04120BOX and NW04122BOX; Thermo Fisher Scientific, Inc.) for SDS-PAGE and then transferred onto nitrocellulose membranes (cat. no. 10600002; GE Healthcare). The membranes were blocked with 5% skim milk (cat. no. 232100; Difco; BD Biosciences) in TBST (0.05% Tween 20) at room temperature for 1 h and then incubated with primary antibodies at 4˚C overnight. Next, the membranes were washed with TBST three times and incubated with secondary antibodies at room temperature for 1 h. After the membranes were washed with TBST a further three times, they were treated with ECL Select Western blot detection reagent (cat. no. RPN2235; Cytivia).

Target proteins were detected using a Fusion FX5 image analyzer (Vilber Lourmat). The normalized relative protein levels (compared with the respective actin bands) were calculated using ImageJ software (version 1.53k; National Institutes of Health). Information regarding the antibodies used for western blotting is provided in Table SIII.

Cytotoxicity assay. Cells were treated with 5 μM 2',7'-bis-(2-carboxyethyl)-5-(and-6)-carboxyfluorescein, acetoxymethyl ester (BCECF, AM; cat. no. B1150; Thermo Fisher Scientific, Inc.) for 30 min at 37˚C and subsequently harvested in a 1 ml tube. The cells were then washed with sodium veronal buffer (cat. no. B102; Complement Technology, Inc.) and treated with normal human serum (NHS; cat. no. NHS; Complement Technology, Inc.) or 1% SDS (cat. no. 28312; Thermo Fisher Scientific, Inc.) in veronal buffer (as a positive control) for 30 min at 37˚C. Next, the sample supernatants were transferred to black 96-well plates and the fluorescence was measured (excitation, 485 nm; emission, 538 nm). The cytotoxicity was calculated using the following formula: Cytotoxicity=[(A-B)/(C-B)] x100%. Where A is the BCECF released from the samples, B is the spontaneous BCECF and C is the BCECF released from the SDS positive control.

ELISA. ELISAs were performed on the cells using the Human Complement Component C5a DuoSet ELISA kit (cat. no. DY2037; R&D Systems, Inc.) according to the manufacturer's protocols. The optical density of the samples at 450 nm was measured using a microtiter plate spectrophotometer (Beckman Coulter, Inc.).

Irradiation. Cells were exposed to γ-rays using a ^{137}Cs-ray source (Eckert & Ziegler) at a dose rate of 2.6 Gy/min. Following irradiation at doses of 0, 2, 4 and 6 Gy, the cells were incubated for 24 h at 37˚C in a humidified incubator with 5% CO_2.

Clonogenic cell survival assay. Cells were irradiated as aforementioned. The cells were then seeded in 6-well culture plates at a density of 500 cells/well for 10 days at 37˚C, in a humidified incubator with 5% CO_2. Following incubation, the colonies were fixed with 2 ml ice-cold methanol for 10 min at 4˚C, and were stained with a 1% crystal violet solution in methanol at room temperature for 1 h. After washing with distilled water, the colonies, which contained at least 50 cells, were counted manually.

Mammosphere formation assay. Cells were irradiated as aforementioned. Following exposure to ionizing radiation, the non-irradiated or irradiated cells were detached from the plate with TrypLE Express (cat. no. 12605-010; Gibco; Thermo Fisher Scientific, Inc.) and reseeded at a density of 100 cells/well in ultra-low-attachment surface spheroid 96-well microplates (cat. no. 4520; Corning, Inc.) in MammoCult Human Medium (cat. no. 05620; Stemcell Technologies, Inc.) supplemented with a heparin solution and hydrocortisone stock solution (cat. nos. 07980 and 07925, respectively; Stemcell Technologies, Inc.). The suspended cells were incubated for 7-14 days at 37˚C in a humidified incubator with 5% CO_2. Mammosphere formation was monitored, and the sphere size was measured using the following formula: Sphere size=(long diameter + short diameter)/2.

Cell migration and invasion assays. Cells were irradiated as aforementioned. Transwell inserts (8-μm pore size; cat. no. 353097; Falcon; Corning Life Sciences) were coated with a collagen solution (cat. no. C2249-20ML; Sigma-Aldrich; Merck KGaA) or Matrigel (for the invasion assay; cat. no. 354230; Corning, Inc.) and placed into 24-well microplates containing 800 μl complete medium and 10% FBS. The cells were suspended in serum-free medium at a density of 5x10^4 cells/150 μl and seeded on each membrane insert. After incubation for 20 h at 37˚C in a humidified incubator with 5% CO_2, the inserts were washed with PBS and fixed with ice-cold methanol at 4˚C for 10 min. Then, the inserts were stained with a 1% crystal violet solution in methanol at room temperature for 1 h. After washing with distilled water, cells that had not migrated to the upper membrane of the insert were removed using a cotton swab. The migrated or invaded cells were observed using an EVOS XL Cell Imaging System (Thermo Fisher Scientific, Inc.) at x100 magnification.

Flow cytometry. Cells were irradiated as aforementioned. The cells were then washed with 1X DPBS, harvested by centrifuging at 1,200 rpm (335 x g) for 3 min at 4˚C and then fixed with 70% cold ethanol for 1 h at 4˚C. The fixed cells were washed with 1X DPBS and stained with PI solution for 30 min at 4˚C. The stained cells were then washed and resuspended in 500 μl BD FACS™ Sheath Fluid (cat. no. 342003; BD biosciences), and the cell cycle was analyzed using a BD FACSAria Cell Sorter Special Order Research Product (BD Biosciences) and BD FACSDiva Software (version 6.1.3; BD Biosciences).

For the Annexin V apoptosis assay, the fixed cells were washed with 1X DPBS and stained with FITC Annexin V from a FITC Annexin V Apoptosis Detection Kit I (cat. no. 556547; BD Biosciences) in 1X binding buffer (from the aforementioned kit). The cells labeled with FITC Annexin V were stained with a PI solution and analyzed using BD FACSAria Cell Sorter Special Order Research Product (BD Biosciences) and BD FACSDiva Software.

Gene expression profiling and function analysis. Total RNA was isolated from NS and CFH knockdown MDA-MB-231 cells using a Ribospin RNA purification kit. A total of six samples (three NS and three CFH knockdown cell lines) were chosen for microarray analysis to predict the association between downregulated CFH gene expression and breast cancer. cDNA was synthesized using the GeneChip WT Amplification kit (cat. no. 902230; Thermo Fisher Scientific, Inc.), as described by the manufacturer. The Affymetrix GeneChip Human Gene 2.0 ST Array platform was used for microarray analysis and scanned on a GCS3000 Scanner (Affymetrix; Thermo Fisher Scientific, Inc.). The following filtering criteria were used to define differentially expressed genes (DEGs): A change in gene expression by >2-fold and P<0.01. The QuickGO database was used to classify categories enriched in the DEGs with comparable functions (GO analysis, https://www.ebi.ac.uk/QuickGO/annotations;TOPPFUNanalysis, https://toppgene.cchmc.org/enrichment.jsp; DAVID analysis,

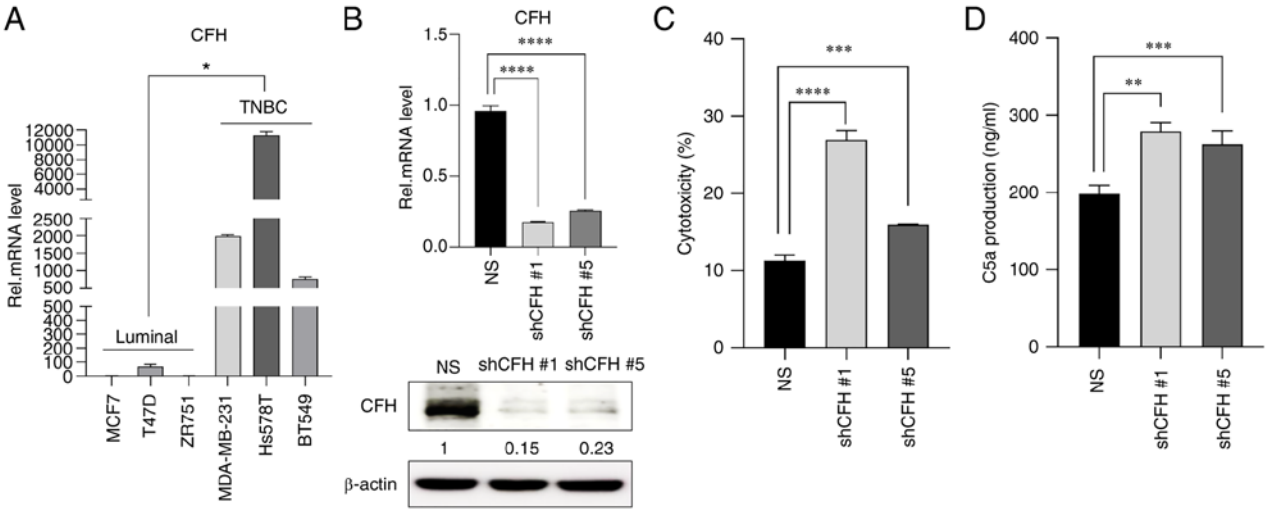

Figure 1. CFH knockdown in MDA-MB-231 reduces the ability to defend against CDC. (A) CFH mRNA expression levels in luminal (MCF7, T47D and ZR751) and TNBC (MDA-MB-231, Hs578T and BT549) human breast cancer cell lines were analyzed by RT-qPCR. The results are presented as the mean ± SD. *P<0.05 luminal vs. TNBC, using the unpaired Student's t test. (B) MDA-MB-231 cells were transfected with NS, shCFH #1 or shCFH #5, and downregulated expression was measured by RT-qPCR and western blotting. The expression levels were semi-quantified and defined beneath each protein band. The expression levels were calculated as the target/b-actin ratio for each lane and the ratio values for the experimental group were normalized by setting the ratio value of the negative control group to 1. (C) A CDC assay was performed by measuring 2',7'-bis-(2-carboxyethyl)-5-(and-6)-carboxyfluorescein, acetoxymethyl ester release induced by normal human serum from NS and shCFH transfected cells. (D) C5a production was measured using a commercially available C5a detection ELISA kit. The results are presented as the mean ± SD. *P<0.05, **P<0.01, ***P<0.001, ****P<0.0001, using one-way ANOVA and Tukey's test. CDC, complement-dependent cytotoxicity; CFH, complement factor H; NS, non-silencing shRNA; Rel, relative; RT-qPCR, reverse transcription-quantitative PCR; sh(RNA), short hairpin (RNA); TNBC, triple-negative breast cancer.

https://david.ncifcrf.gov/). The raw dataset has been uploaded to the ArrayExpress database (accession no. E-MTAB-13327).

Small interfering RNA (siRNA) knockdown. MDA-MB-231 cells or shCFH #1 cells in 6-well plates containing 2 ml Opti-MEM (cat. no. 31985-070; Gibco; Thermo Fisher Scientific, Inc.) were transfected with a mixture containing 20 nM universal negative control (NC) siRNA or 20 nM erythrocyte membrane protein band 4.1-like 3 (EPB41L3)-targeting siRNA (TriFECTa DsiRNA kit; cat. no. hs.Ri.EPB41L3.13; Integrated DNA Technologies, Inc.) and 4 μl jetPRIME Transfection Reagent (cat. no. 101000046; Polyplus-transfection SA) in 200 μl of jetPRIME buffer (Polyplus-transfection SA) for 24 h at 37˚C in a humidified incubator with 5% CO_2. Subsequent experiments were performed after 24 h incubation. Information regarding the siRNAs used for EPB41L3 knockdown is provided in Table SIV.

Statistical analysis. All experiments were repeated at least three times. GraphPad Prism 8 software (Dotmatics) was used for all statistical analyses. Data are presented as the mean ± standard deviation. Analyses were performed with unpaired Student's t-test, or one-way or two-way ANOVA followed by Tukey's test. P<0.05 was considered to indicate a statistically significant difference.

Results

CFH downregulation sensitizes MDA-MB-231 cells against complement-dependent cytotoxicity (CDC). The CFH expression levels in various breast cancer cell lines were investigated to evaluate the basal levels in luminal and triple-negative breast cancer (TNBC) subtypes. Notably, the TNBC group exhibited significantly higher CFH expression than the luminal group (Fig. 1A). Next, stable CFH knockdown cells were established through shRNA viral transfection into TNBC MDA-MB-231 cells (cells that are highly aggressive with high metastatic potential). It was confirmed that CFH expression was downregulated in MDA-MB-231 cells transfected with shCFH #1 and #5 (Figs. 1B and S1). To examine the effect of CFH downregulation on the inhibitory function of NHS containing complement proteins, cytotoxicity assays and a C5a ELISA were performed. The cytotoxicity and level of C5a release induced by NHS were significantly increased in cells transfected with shCFH #1 and #5 compared with NS cells (Fig. 1C and D). Therefore, these data demonstrated that CFH knockdown inhibited the protection against immune attack by complement proteins in MDA-MB-231 cells.

CFH downregulation decreases cell survival and suppresses motility by decreasing radioresistance and promotes apoptosis through G2/M phase cell cycle arrest. Experiments were performed to investigate whether CFH downregulation could decrease the radioresistance and survival of MDA-MB-231 cells. Irradiated cells were seeded onto 6-well plates and incubated for 7-10 days. Notably, the number of shCFH #1 cell colonies following irradiation was significantly reduced compared with that of NS cells in a dose-dependent manner (Fig. 2A and B). Next, to examine whether CFH could affect anchorage-independent properties, irradiated cells were cultured on 96-well plates for 7-10 days to develop mammospheres. The size of the CFH mammospheres was decreased compared with that of the NS cell mammospheres (Fig. 2C and D). Furthermore, the effect of CFH knockdown on cell motility was evaluated through migration and invasion assays. Notably, the relative migration and invasion of irradiated shCFH #1 cells

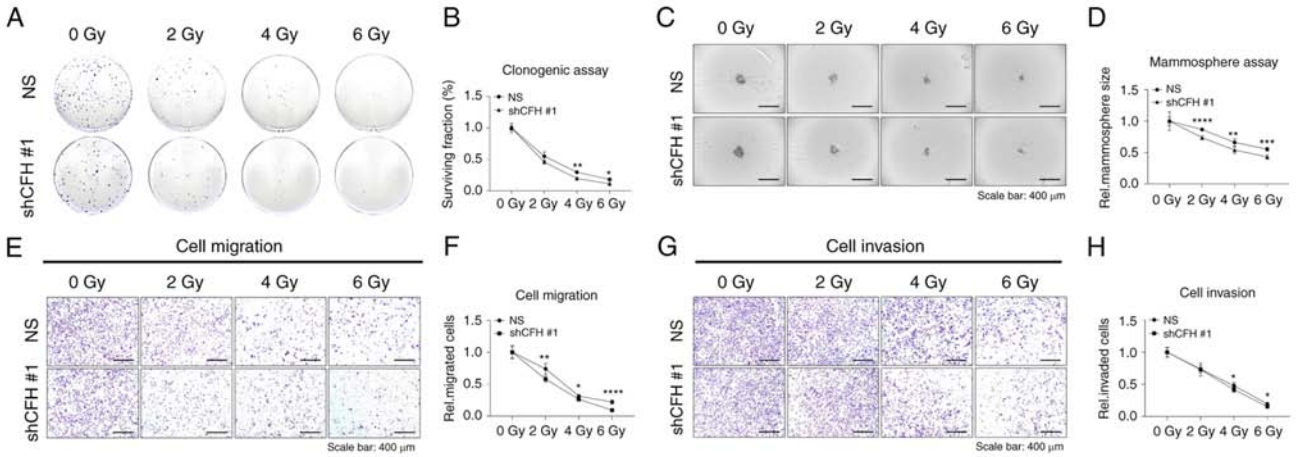

Figure 2. CFH knockdown suppresses the aggressive phenotypes of MDA-MB-231 cells by increasing radiosensitivity. (A) A clonogenic assay was performed using a crystal violet solution after irradiation and (B) the surviving fraction was measured by counting the colonies. (C) A mammosphere formation assay was performed using an ultra-low-attachment plate and MammoCult Human Medium kit supplemented with a heparin solution and hydrocortisone stock solution. Mammosphere size was observed and measured using a microscope and (D) quantified. (E) A cell migration assay was performed using Transwell inserts with an 8 mm pore size coated with collagen, and cells were stained with a crystal violet solution. (F) The migrated cells were measured by counting the stained cells. (G) A cell invasion assay was performed using Transwell inserts with an 8-mm pore size coated with Matrigel, and cells were stained with a crystal violet solution. (H) The invaded cells were measured by counting the stained cells. The results are presented as the mean ± SD. *P<0.05, **P<0.01, ***P<0.001, ****P<0.0001 NS vs. shCFH #1. Analyses were performed with unpaired Student's t test. CFH, complement factor H; NS, non-silencing shRNA; Rel, relative; sh(RNA), short hairpin (RNA).

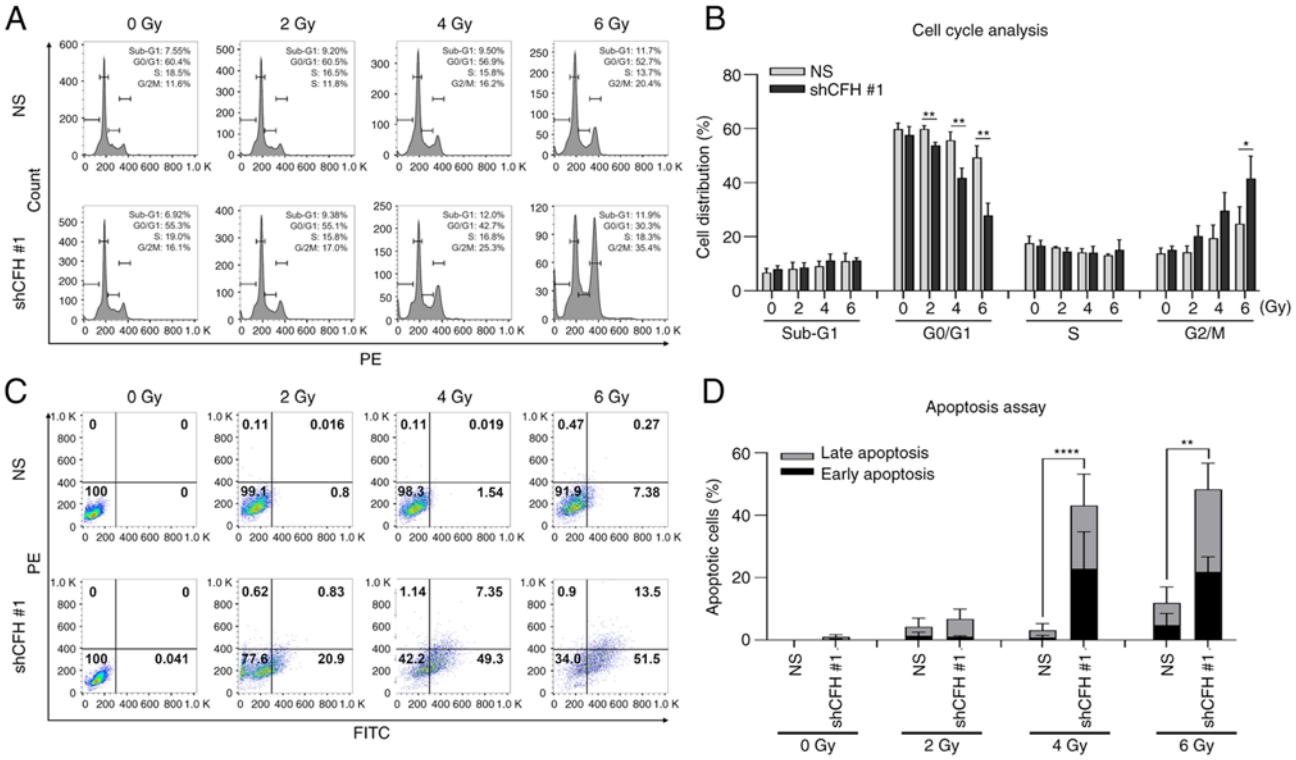

Figure 3. CFH knockdown accelerates apoptosis through G2/M phase cell cycle arrest by radiation. (A) Cell cycle analysis was performed using flow cytometry and was (B) quantified. (C) Apoptosis analysis was performed using flow cytometry and was (D) quantified. The results are presented as the mean ± SD. *P<0.05, **P<0.01, ****P<0.0001, using the unpaired Student's t test. CFH, complement factor H; NS, non-silencing shRNA; PE, phycoerythrin; Rel, relative; sh(RNA), short hairpin (RNA).

were decreased compared with those of irradiated NS cells (Fig. 2E-H). Additionally, cell cycle analysis and an apoptosis assay using flow cytometry were performed following cell irradiation. The ratio of shCFH #1 cells arrested in G2/M phase increased with irradiation (Fig. 3A and B), and these cells showed a significantly increased apoptotic cell ratio compared with that of the NS cells (Fig. 3C and D). These results indicated that CFH downregulation suppressed cell survival and motility and promoted apoptosis through G2/M phase cell cycle arrest by sensitizing breast cancer cells to radiation.

CFH downregulation alters the expression levels of multiple genes associated with BCSCs. The specific characteristics of CSCs might be maintained through their enhanced survival, motility and radioresistance through gene expression regulation. To explore whether CFH can regulate the expression of various genes associated with BCSCs, RT-qPCR was performed to measure the levels of BCSC marker genes. Compared with the NS cells, the shCFH #1 cells showed increased CD24 expression and decreased CD44 and CD133 expression, indicating the loss of the typical phenotype for BSCS cells, such as having a $CD24^{low}/CD44^{high}$ population (Fig. 4A). Additionally, the expression levels of Oct4, Sox2, c-Myc and epithelial cellular adhesion molecule (EpCAM) were decreased in shCFH #1 cells compared with NS cells. Moreover, it was found that the differences in protein levels of these genes were similar to the changes in mRNA levels (Figs. 4B and S2). These results demonstrated that CFH knockdown decreased the CSC properties related to radioresistance by regulating gene expression in breast cancer cells.

Next, microarray expression profiling was performed to identify genes regulated by decreased CFH expression (Fig. 4C). It was found that the DEGs were associated with motility, growth, signal transduction and, in particular, breast cancer. Based on these analyses, 25 genes were selected as candidate hub genes that may interact with numerous other genes. As such, the biological functions, regulatory mechanisms and signaling pathways of the 25 genes in cancer cells were further investigated and the diverse characteristics of the 25 genes in cancer were verified through bioinformatic analysis. Then, seven genes that had a high correlation with survivability, motility, radioresistance and cancer stemness were selected. The selected seven genes were endothelial PAS domain protein 1, cyclin-dependent kinase inhibitor 1B, protein tyrosine phosphatase receptor type J and EPB41L3, which showed increased expression due to CFH downregulation, and myosin VI, gap junction protein α1 and C-X-C motif chemokine receptor 4 (CXCR4), which exhibited decreased expression. Taken together, these microarray findings indicated that several genes were regulated by CFH knockdown and allowed for the selection of target genes. A list of gene ontology terms is provided in Tables SV-VIII.

CFH downregulation attenuates CSC characteristics via the regulation of MAPK signaling by upregulating EPB41L3 in MDA-MB-231 breast cancer cells. A total of seven notable genes that were differentially expressed in NS and shCFH #1 cells were identified (Fig. 5A). Of these genes, CXCR4 is a tumor promoter and EPB41L3 plays a role in tumor suppression. CXCR4, a widely expressed oncogenic factor in malignant solid tumors, is correlated with cancer progression, invasion, DNA repair, radioresistance and CSC properties, and is involved in survival or oncogenic signaling pathways, including STAT3, MAPK, PI3K/AKT and sonic hedgehog (27,28). By contrast, EPB41L3 inhibits invasion, metastasis and tumor development in various cancer cells, such as breast, ovarian, prostate and gastric cancer cells, and induces apoptosis (29,30). Therefore, CXCR4 and EPB41L3, which exhibited significant expression changes following CFH knockdown, were selected as candidate factors for further validation.

To investigate whether CFH knockdown affected the CXCR4 or EPB41L3 signaling cascade, CXCR4- or EPB41L3-associated protein phosphorylation were examined using western blotting. First, the CXCR4/ Janus kinase (JAK)/STAT3 signaling pathway, a major oncogenic cascade in CSCs (27,28), was analyzed. However, the phosphorylation levels of JAK1, JAK2 and STAT3 were not affected by CFH knockdown (Figs. 5B and S3). Next, the tumor suppressor protein, EPB41L3, which is involved in the PI3K/AKT and MAPK pathways (29,30), was analyzed. For this, whether increased EPB41L3 expression could regulate the phosphorylation levels of AKT, ERK, JNK and p38 MAPK was explored. Notably, phosphorylated-ERK (p-ERK) levels were reduced and p-p38 levels were significantly increased in shCFH #1 cells, which contained upregulated EPB41L3 expression following CFH knockdown, compared with NS cells (Figs. 5C and S4).

Moreover, after analyzing the METABRIC breast cancer and TNBC data, it was demonstrated that the patient groups with high EPB41L3 expression had an improved survival rate compared with the low expression groups (Fig. 5D). However, the results of the analysis of the TNBC data were not statistically significant. In addition, the survival rates of patients with breast cancer were further analyzed according to the levels of EPB41L3 expression in the CFH high and CFH low expression cohorts (Fig. 5E). In the CFH low expression cohort, the EPB41L3 high expression cohort had a slightly higher survival rate than the EPB41L3 low expression cohort, but this result was not statistically significant. These results indicated that the EPB41L3 expression level may influence the survival rates of patients with breast cancer. However, the correlation with CFH was not statistically significant.

EPB41L3 downregulation restores cell survival, migration and invasion abilities through the enhancement of radioresistance via the regulation of MAPK signaling in MDA-MB-231 breast cancer cells. It was next investigated whether the re-downregulation of EPB41L3, which was upregulated by CFH suppression, could rescue the CFH suppression effect. To confirm the downregulation of EPB41L3 siRNA, MDA-MB-231 cells were transfected with universal NC siRNA or siEPB41L3-#1, -#2 and -#3, and RT-qPCR and western blotting were performed (Figs. 6A and S5). Moreover, EPB41L3 downregulation by siEPB41L3 #2 in shCFH #1 cells induced an increase in p-ERK and a decrease in p-p38 levels compared with shCFH #1 or NC cells (Figs. 6B and S6). In accordance with these results, it was next examined whether reactivation of the signaling pathways induced by downregulation of EPB41L3 could transform cancer cells to aggressive phenotypes. shCFH #1 cells were irradiated following transfection with NC or EPB41L3 #2 siRNA, and then clonogenic, migration and invasion assays were performed. Compared with shCFH #1 or NC cells, the shCFH #1 + siEPB41L3 #2 cells showed increased survival and motility upon radiation treatment (Fig. 6C-E). These data demonstrated that upregulation of the EPB41L3 tumor suppressor by CFH knockdown increased the radiotherapy sensitivity of MDA-MB-231 cells through the decrease of radioresistance via MAPK regulation. Consequently, CFH downregulation suppressed the expression of CSC-associated genes via the regulation of ERK and p38 MAPK signaling by increasing EPB41L3 protein expression.

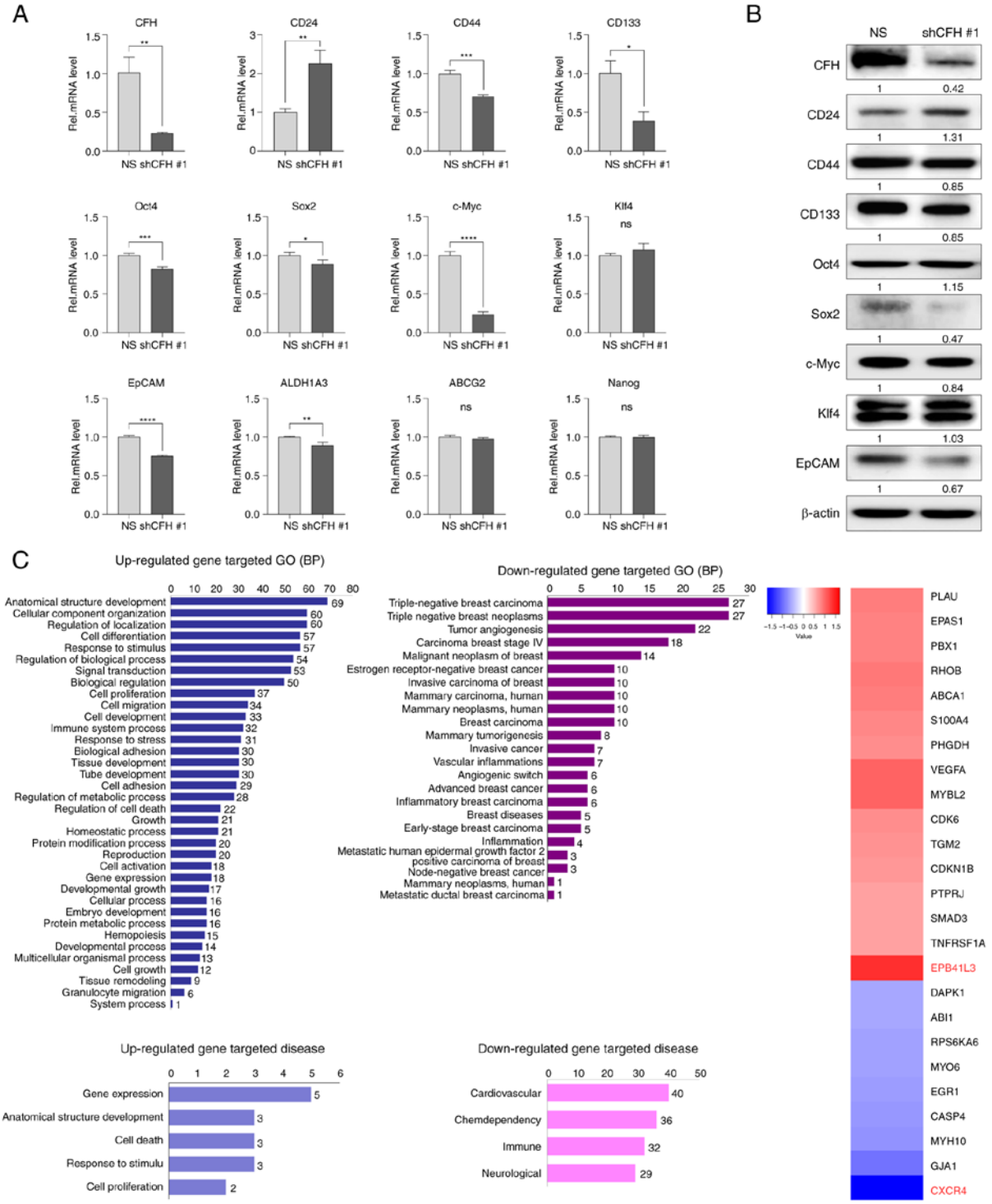

Figure 4. CFH knockdown controls the expression patterns of BCSC-associated genes. The expression levels of BCSC-specific and stemness-related genes were analyzed by (A) reverse transcription-quantitative PCR and (B) western blotting, following irradiation and shRNA transfection. The expression levels were semi-quantified and defined beneath each protein band. The expression levels were calculated as the target/b-actin ratio for each lane and the ratio values for the experimental group were normalized by setting the ratio value of the negative control group to 1. (C) Gene expression profiling identified several pro- or antitumor genes as major candidate downstream factors of the CFH signaling mechanism, through BP, disease and heatmap analyses using bioinformatics tools. The results are presented as the mean ± SD. *P<0.05, **P<0.01, ***P<0.001, ****P<0.0001, using an unpaired Student's t test. ABCG2, ATP biding cassette subfamily G member 2; ALDH1A3, aldehyde dehydrogenase 1 family member A3; BCSC, breast cancer stem cell; BP, biological process; CFH, complement factor H; EpCAM, epithelial cellular adhesion molecule; GO, Gene Ontology; Klf4, Klf transcription factor 4; NS (uppercase), non-silencing shRNA; ns (lowercase), not significant; Rel, relative; sh(RNA), short hairpin (RNA).

Discussion

The complement cascade protects the body against diverse pathogens. This process is accompanied by the release of inflammatory factors, such as interleukins, IFN-γ, TNF-α and TGF-β, from mast cells, monocytes, macrophages, peripheral blood mononuclear cells, antigen-presenting cells and T cells. These cells and cytokines control the immune response by

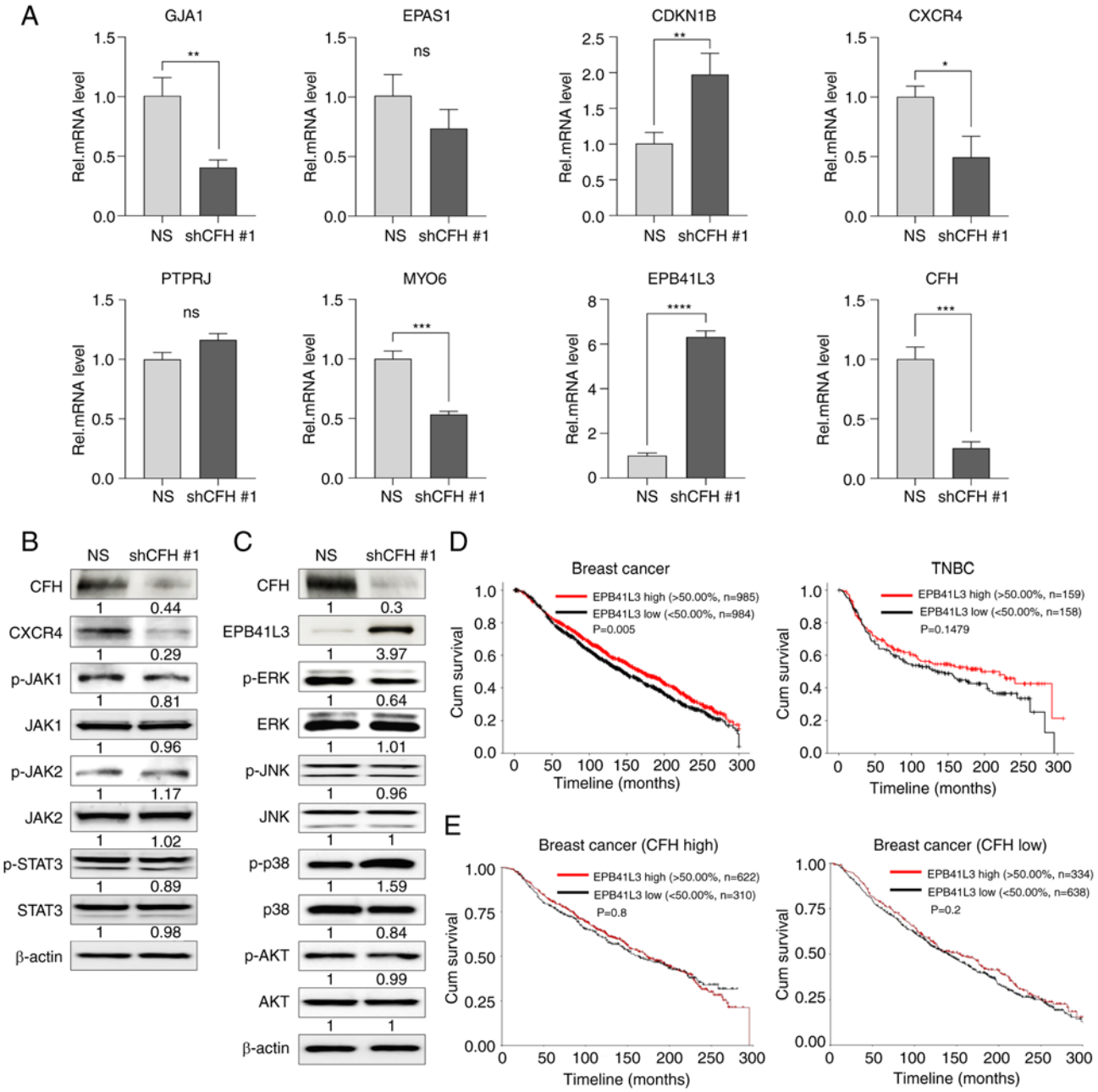

Figure 5. CFH knockdown regulates the MAPK signaling pathway by increasing EPB41L3 expression. (A) The mRNA expression levels of seven major candidate genes were measured by reverse transcription-quantitative PCR. The results are presented as the mean ± SD. *P<0.05, **P<0.01, ***P<0.001, ****P<0.0001, using an unpaired Student's t test. The expression levels of (B) CXCR4 and (C) EPB41L3 signaling pathway proteins were analyzed by western blotting. The expression levels were semi-quantified and defined beneath each protein band. The expression levels were calculated as the target/b-actin ratio for each lane and the ratio values for the experimental group were normalized by setting the ratio value of the negative control group to 1. (D) Correlation between the EPB41L3 expression level and the survival rate of patients with all types of breast cancer or TNBC was analyzed using METABRIC data using the log-rank test. The results were validated using the Cox proportional hazards model. (E) Correlation of the survival rates of patients with breast cancer according to the level of EPB41L3 expression in the CFH high or low expression cohorts. This analysis utilized the survival and survminer packages in R for conducting survival analysis, and was validated using the Cox proportional hazards model. CDKN1B, cyclin-dependent kinase inhibitor 1B; CFH, complement factor H; CXCR4, C-X-C motif chemokine receptor 4; EPAS1, endothelial PAS domain protein 1; EPB41L3, erythrocyte membrane protein band 4.1-like 3; GJA1, gap junction protein α1; JAK, Janus kinase; METABRIC, Molecular Taxonomy of Breast Cancer International Consortium; MYO6, myosin VI; NS (uppercase), non-silencing; ns (lowercase), not significant; PTPRJ, protein tyrosine phosphatase receptor type J; shRNA; Rel, relative; sh(RNA), short hairpin (RNA); TNBC, triple-negative breast cancer.

interacting and communicating with each other. However, if this process is not terminated and instead maintained continuously, it can generate chronic inflammation and a favorable environment for tumors. In fact, the sublytic pore of the cell membrane is known to trigger tumor progression by promoting chronic inflammation (14,31). Therefore, cancer cell death should be induced through an effective immune response to prevent a chronic inflammatory environment.

Human breast cancer cells are classified into several types, such as luminal A and B, HER2^{+} and TNBC cells. TNBC cells are difficult to completely eliminate despite advanced drug and radiotherapy techniques due to their high capacities for

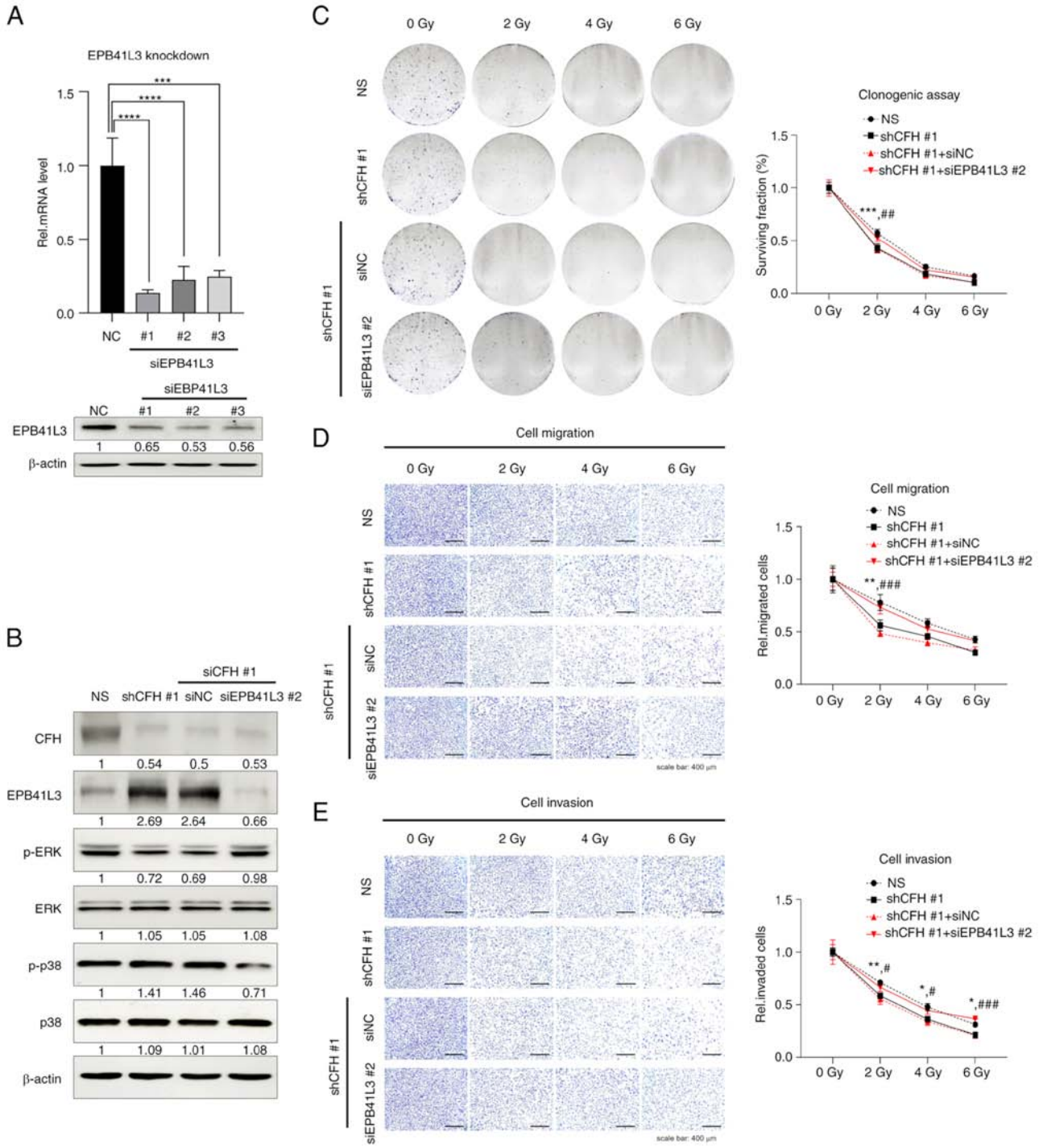

Figure 6. EPB41L3 knockdown may eliminate the effect of CFH suppression on cell survival, migration and invasion abilities. (A) MDA-MB-231 cells were transfected with NC, EPB41L3 #1, #2 or #3. The mRNA and protein expression levels of EPB41L3 were measured by reverse transcription PCR and western blotting. The results are presented as the mean ± SD. ***P<0.001, ****P<0.0001, using one-way ANOVA and Tukey's test. (B) The phosphorylation levels of ERK and p38 MAPK were confirmed by western blotting following NC or siEPB41L3 #2 transfection. The expression levels were semi-quantified and defined beneath each protein band. The expression levels were calculated as the target/b-actin ratio for each lane and the ratio values for the experimental group were normalized by setting the ratio value of the negative control group to 1. (C) A clonogenic assay was performed using a crystal violet solution after NC or siEPB41L3 #2 transfection and irradiation. The surviving fraction was measured by counting the colonies. (D) Cell migration and (E) invasion assays were performed using Transwell inserts with an 8-μm pore size coated with collagen or Matrigel, and cells were stained with a crystal violet solution. NC or siEPB41L3 #2 transfected cells were irradiated. The results are presented as the mean ± SD. *P<0.05, **P<0.01, ***P<0.001 NS vs. shCFH #1; $^{\#}$P<0.05, $^{\#\#}$P<0.01, $^{\#\#\#}$P<0.001 shCFH #1 + siNC vs. shCFH #1 + siEPB41L3 #2, using two-way ANOVA and Tukey's test (the two variables were presence of gene regulation and the radiation dose). CFH, complement factor H; EPB41L3, erythrocyte membrane protein band 4.1-like 3; EpCAM, epithelial cellular adhesion molecule; NC, negative control; NS, non-silencing; p-, phosphorylated; Rel, relative; sh(RNA), short hairpin (RNA); si(RNA), small interfering (RNA).

survival, invasion and radioresistance, which lead to metastasis and recurrence (32). BCSCs can exhibit various phenotypes by maintaining high expression levels of CD44 and CD133, which enhance stemness, cell survival, growth, migration, invasion, chemoresistance and radioresistance through signaling pathways such as NF-κB, cAMP response element-binding

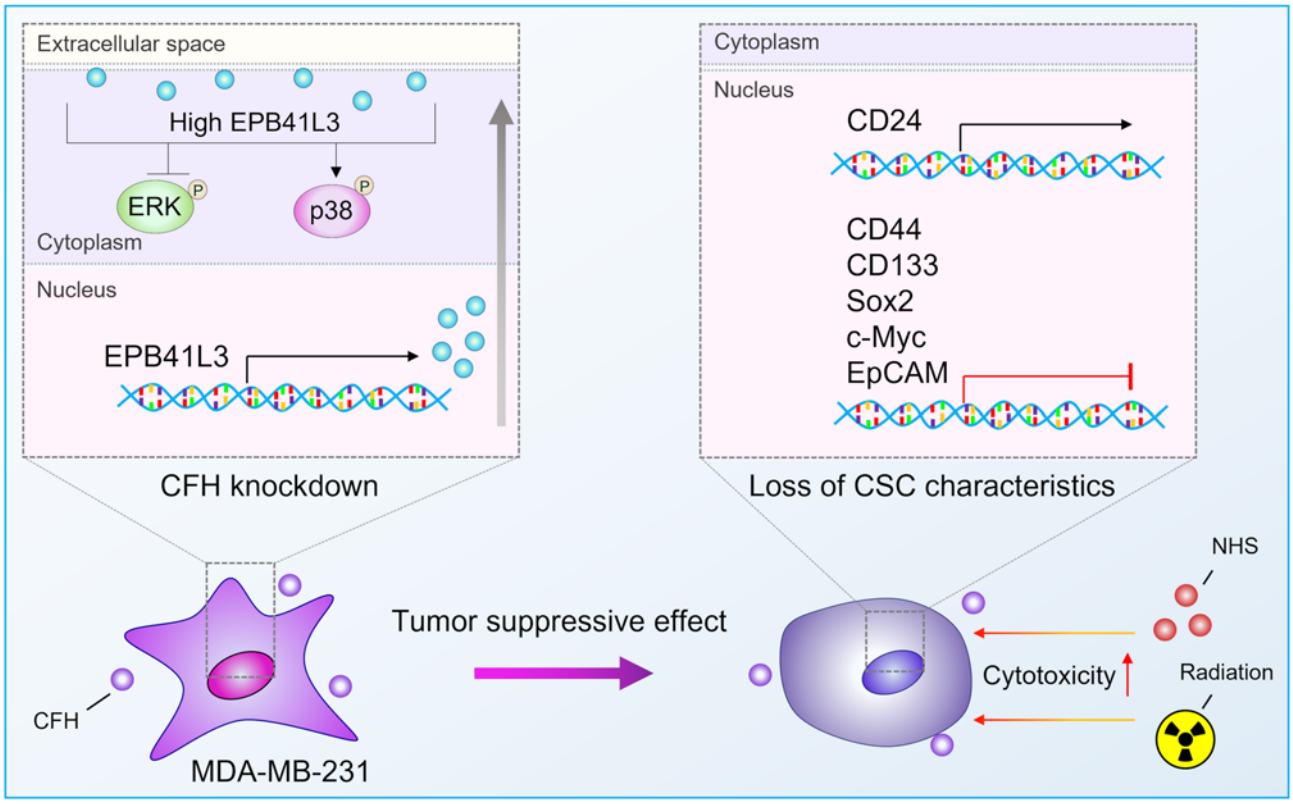

Figure 7. CFH knockdown suppresses the stemness of breast cancer cells through regulation of the EPB41L3/MAPK axis. CFH downregulation induced EPB41L3 expression, which induced the inhibition of ERK and the activation of the p38 signaling pathway. It also regulated related genes to decrease BCSC characteristics and trigger a decrease in resistance to immune attack and irradiation in MDA-MB-231 human breast cancer cells. BCSCs, breast cancer stem cells; CFH, complement factor H; EPB41L3, erythrocyte membrane protein band 4.1-like 3; NHS, normal human serum.

protein/TGF-β2, β-catenin and IL-6/Notch3 (33-36). For these reasons, the discovery of targets to suppress cancer stemness is crucial to prevent recurrence and metastasis and improve therapeutic efficacy. According to a report, suppressor of cytokine signaling-1 and -3/JAK/STAT4, an oncogenic transcription factor pathway, increases the expression of CFH in A549 lung cancer cells (37). Moreover, intracellular CFH overexpression promotes proliferation, migration and survival independent of the complement cascade in A498 renal cancer cells and A549 cells (20). Additionally, CFH uptake controls intracellular C3 activation in apoptotic cells and represses the inflammatory potential of released nucleosomes (38). However, to the best of our knowledge, the distinct role of intracellular CFH in cancer cells is not known. According to a recent study, CFH in exosomes released from metastatic hepatocellular carcinoma cells induced tumorigenesis and metastasis by increasing cell growth, migration and invasiveness (39). More notably, CFH expressed by breast cancer cells promotes the differentiation of $CD14^+$ monocytes into immunosuppressive macrophages (23). These studies suggest that CFH may affect tumor progression and the maintenance of stemness potential through direct regulation of specific genes and indirect interaction with their surrounding microenvironments, including various immune cells (23,38,39). Therefore, we hypothesize that CFH is a target factor to enhance the effectiveness of drugs and radiotherapy by suppressing stemness and aggressive phenotypes.

Indeed, the microarray results of the present study demonstrated that numerous genes regulated by CFH knockdown were involved in breast cancer. These genes were associated with essential biological processes for survival, including proliferation, growth, migration and signal transduction. CXCR4, a major pro-tumor receptor that promotes signal transduction by binding the CXCL12 ligand, is upregulated in a number of cancer types. The upregulation of CXCR4 in the tumors of patients with TNBC is known to promote tumor growth and metastasis, and upregulated CXCR4 is also associated with proliferation, motility and metastasis in colon and gastric cancer (40-42). In the present study, CXCR4 expression was suppressed by CFH knockdown but this did not affect the downstream signaling of CXCR4. The CXCR4 downstream pathway, JAK/STAT3, is likely to be activated by alternative ligands including EGF, IL-10, IL-6 and IL-11. (43) By contrast, EPB41L3 is a potential antitumor gene that plays a key role in cytoskeletal organization and remodeling and participates in diverse biological processes through its interaction with cytoplasmic or membrane proteins via the four one-ezrin-radixin-moesin domain (29). According to a previous study, EPB41L3 overexpression represses proliferation and induces apoptosis in esophageal squamous cell carcinoma cells through G2/M arrest (44). In addition, EPB41L3 inhibited osteosarcoma cell invasion through the suppression of epithelial-mesenchymal transition induced by snail-1 (30). The results of the present study corroborate the antitumor role of EPB41L3 and its related signaling pathway.

The activation of ERK plays a radioprotective function by enhancing Bcl-2 and p65 expression while repressing Bax

and p53 expression (45). Lapatinib, an EGFR/HER2 kinase inhibitor, induces radiosensitization through the inhibition of ERK (46). Furthermore, the p38 signaling pathway enhances radiosensitivity by increasing G2/M phase arrest and apoptosis through the suppression of cyclin B1, CDK1 and Bcl-2 (47). Activation of the p38 signaling pathway promotes apoptosis by regulating the Bax/Bcl-2/caspase-3, -7 and -9 cascade and induces cell cycle arrest through the suppression of CDK2, CDK4, cyclin D1 and cyclin E1 (48,49). As is well-known, the ERK and p38 signaling pathways play a crucial role as key mediators in regulating multiple phenotypes of cancer cells. The results of the present study revealed that CFH could enhance stemness, which is associated with malignant phenotypes and chemoresistance and radioresistance, through the regulation of the EPB41L3/ERK/p38 signaling pathway. It was demonstrated in the present study that downregulation of CFH, which regulates the activity of MAPKs and suppresses stemness-related phenotypes (such as $CD24^{-}/CD44^{+}$, $CD133^{+}$ and $EpCAM^{+}$), enhanced radiosensitivity, thereby reducing cell survival and motility due to irradiation-induced damage. Additionally, CFH-knock down cells with increased radiosensitivity underwent cell cycle arrest upon irradiation, leading to a higher level of apoptotic signals. Collectively, these results demonstrated that downregulation of CFH in MDA-MB-231 cells increased the expression of the EPB41L3 tumor suppressor, suppressed ERK activation, promoted p38 activation, suppressed cancer stemness and enhanced irradiation-induced damage.

A future study stemming from the present study would be to analyze the level of complement activation and CDC as well as the tumor suppression effect of CFH downregulation through tumor xenograft experiments. However, it is difficult to select a suitable mouse model with a normal immune system that can be used for xenografting as the structural differences in complement factors between humans and mice might lead to inaccurate experimental data related to abnormal activation of complement responses, such as hyperactivation or inactivation. Therefore, ways to develop a proper mouse model through CRISPR-Cas technology and humanized mouse models are being studied. In the future, the correlation of the complement system and human breast cancer will be studied using a mouse model that is currently in development.

In conclusion, CFH downregulation suppressed the expression of BCSC-specific genes by promoting EPB41L3 expression via regulation of the MAPK signaling pathway in MDA-MB-231 breast cancer cells (Fig. 7). Additionally, since CFH downregulation promoted the activation of CDC, it might contribute to overcoming many side effects of anticancer therapies by improving therapeutic efficiency. Therefore, CFH is a potential target for efficient radiotherapy for human breast cancer treatment.

Acknowledgements

Not applicable.

Funding

This work was supported by The Dongnam Institute of Radiological & Medical Sciences grant funded by The Korean Government (grant no. 50591-2023).

Availability of data and materials

The datasets generated by microarray are available in the ArrayExpress database (https://www.ebi.ac.uk/biostudies/arrayexpress/studies/E-MTAB-13327?query=E-MTAB-13327). All other datasets used and/or analyzed during the current study are available from the corresponding author on reasonable request.

Authors' contributions

SYP, DYE and YJC designed the study. SYP, DYE, YJ and JWS performed the experiments. CYL analyzed the microarray data. SHC, SJP and KH analyzed and interpreted the data. SYP and YJC wrote the paper. All authors read and approved the final version of the manuscript. SYP and YJC confirm the authenticity of all the raw data.

Ethics approval and consent to participate

Not applicable.

Patient consent for publication

Not applicable.

Competing interests

The authors declare that they have no competing interests.

References

1. Siegel RL, Miller KD and Jemal A: Cancer statistics. CA Cancer J Clin 69: 7-34, 2019.
2. Weigelt B, Peterse JL and van 't Veer LJ: Breast cancer metastasis: Markers and models. Nat Rev Cancer 5: 591-602, 2005.
3. Bai X, Ni J, Beretov J, Graham P and Li Y: Cancer stem cell in breast cancer therapeutic resistance. Cancer Treat Rev 69: 152-163, 2018.
4. Brooks MD, Burness ML and Wicha MS: Therapeutic implications of cellular heterogeneity and plasticity in breast cancer. Cell Stem Cell 17: 260-271, 2015.
5. El-Sahli S and Wang L: Cancer stem cell-associated pathway in the metabolic reprogramming of breast cancer. Int J Mol Sci 21: 9125, 2020.
6. Badve S and Nakshtri H: Breast-cancer stem cells-beyond semantics. Lancet Oncol 13: e43-e48, 2012.
7. Walcher L, Kistenmacher AK, Suo H, Kitte R, Dluczek S, Strauß A, Blaudszun AR, Yevsa T, Fricke S and Kossatz-Boehlert U: Cancer stem cell-Origins and biomarkers: Perspectives for targeted personalized therapies. Front Immunol 11: 1280, 2020.
8. Fultang N, Chakraborty M and Peethambaran B: Regulation of cancer stem cells in triple negative breast cancer. Cancer Drug Resist 4: 321-342, 2021.
9. J O'Conor C, Chen T, González I, Cao D and Peng Y: Cancer stem cells in triple-negative breast cancer: a potential target and prognostic marker. Biomark Med 12: 813-820, 2018.
10. Barzaman K, Karami J, Zarei Z, Hosseinzadeh A, Kazemi MH, Moradi-Kalbolandi S, Safari E and Farahmand L: Breast cancer: Biology, biomarkers, and treatments. Int Immunopharmacol 84: 106535, 2020.
11. Crabtree JS and Miele L: Breast cancer stem cells. Biomedicines 6: 77, 2018.
12. Huang T, Song X, Xu D, Tiek D, Goenka A, Wu B, Sastry N, Hu B and Cheng SY: Stem cell programs in cancer initiation, progression, and therapy resistance. Theranostics 10: 8721-8743, 2020.
13. Franco SS, Szczesna K, Iliou MS, Al-Qahtani M, Mobasheri A, Kobolák J and Dinnyés A: In vitro models of cancer stem cells and clinical applications. BMC Cancer 16: 738, 2016.

14. Afshar-Kharghan V: The role of the complement system in cancer. J Clin Invest 127: 780-789, 2017.
15. Bajic G, Degn SE, Thiel S and Andersen GR. Complement activation, regulation, and molecular basis for complement-related diseases. EMBO J 34: 2735-2757, 2015.
16. Lewis LA, Ram S, Prasad A, Gulatin S, Getzlaff S, Blom AM, Vogel U and Rice PA: Defining targets for complement components C4b and C3b on the pathogenic neisseriae. Infect Immun 76: 339-350, 2008.
17. Parente R, Clark SJ, Inforzato A and Day AJ: Complement factor H in host defense and immune evasion. Cell Mol Life Sci 74: 1605-1624, 2017.
18. Cserhalmi M, Papp A, Brandus B, Uzonyi B and Jozsi M: Regulation of regulators: Role of the complement factor H-related proteins. Semin Immunol 45: 101341, 2019.
19. Seol HS, Lee SE, Song JS, Rhee JK, Singh SR, Chang S and Jang SJ: Complement proteins C7 and CFH control the stemness of liver cancer cells via LSF-1. Cancer Lett 372: 24-35, 2016.
20. Daugan MV, Revel M, Thouenon R, Dargon-Durey MA, Robe-Rybkine T, Torset C, Merle NS, Noé R, Verkarre V, Oudard SM, *et al*: Intracellular factor H drives tumor progression independently of the complement cascade. Cancer Immunol Res 9: 909-925, 2021.
21. Ajona D, Hsu YF, Corrales L, Montuenga LM and Pio R: Down-regulation of human complement factor H sensitizes non-small cell lung cancer cells to complement attack and reduces in vivo tumor growth. J Immunol 178: 5991-5998, 2007.
22. Junnikkala S, Hakulinen J, Jarva H, Manuelian T, Bjørge L, Bützow R, Zipfel PF and Meri S: Secretion of soluble complement inhibitors factor H and factor H-like protein (FHL-1) by ovarian tumour cells. Br J Cancer 87: 1119-1127, 2002.
23. Smolag KI, Mueni CM, Leandersson K, Jirström K, Hagerling C, Mörgelin M, Barlow PN, Martin M and Blom AM: Complement inhibitor factor H expressed by breast cancer cells differentiates $CD14^+$ human monocytes into immunosuppressive macrophages. Oncoimmunology 9: 1731135, 2020.
24. Liu M, Yang YJ, Zheng H, Zhong XR, Wang Y, Wang Z, Wang YG and Wang YP: Membrane-bound complement regulatory proteins are prognostic factors of operable breast cancer treated with adjuvant trastuzumab: A retrospective study. Oncol Rep 32: 2619-2627, 2014.
25. Pereira B, Chin SF, Rueda OM, Vollan HKM, Provenzano E, Bardwell HA, Pugh M, Jones L, Russell R, Sammut SJ, *et al*: The somatic mutation profiles of 2,433 breast cancers refines their genomic and transcriptomic ladnscapes. Nat Commun 7: 11479, 2016.
26. Livak KJ and Schmittgen TD: Analysis of relative gene expression data using real-time quantitative PCR and the 2(-Delta Delta C(T)) method. Methods 25: 402-408, 2001.
27. Liu X, Xiao Q, Bai X, Yu Z, Sun M, Zhao H, Mi X, Wang E, Yao W, Jin F, *et al*: Activation of STAT3 is involved in malignancy mediated by CXCL12-CXCR4 signaling in human breast cancer. Oncol Rep 32: 2760-2768, 2014.
28. Trautmann F, Cojoc M, Kurth I, Melin N, Bouchez LC, Dubrovska A and Peitzsch C: CXCR4 as biomarker for radioresistant cancer stem cells. Int J Radiat Biol 90: 687-699, 2014.
29. Yuan X, Piao L, Wang L, Han X, Zhuang M and Liu Z: Pivotal roles of protein 4.1B/DAL-1, a FERM-domain containing protein, in tumor progression. Int J Oncol 55: 979-987, 2019.
30. Yuan X, Piao L, Wang L, Han X, Tong L, Shao S, Xu X, Zhuang M and Liu Z: Erythrocyte membrane protein band 4.1-like 3 inhibits osteosarcoma cell invasion through regulation of Snai1-induced epithelial-to-mesenchymal transition. Aging 13: 1947-1961, 2020.
31. Vlaicu SI, Tatomir A, Rus V and Rus H: Role of C5b-9 and RGC-32 in cancer. Front Immunol 10: 1054, 2019.
32. Lagadec C, Vlashi E, Donna LD, Dekmezian C and Pajonk F: Radiation-induced reprogramming of breast cancer cells. Stem Cells 30: 833-844, 2012.
33. Kola P, Nagesh PKB, Roy PK, Deepak K, Reis RL, Kundu SC and Mandal M: Innovative nanotheranostics: Smart nanoparticles based approach to overcome breast cancer stem cells mediated chemo- and radioresistances. Wiley Interdiscip Rev Nanomed Nanobiotechnol 15: e1876, 2023.
34. Jain V, Kumar H, Anod HV, Chand P, Gupta NV, Dey S and Kesharwani SS: A review of nanotechnology-based approaches for breast cancer and triple-negative breast cancer. J Control Release 326: 628-647, 2020.
35. Song K and Faraneh M: Signaling pathways governing breast cancer stem cells behavior. Stem Cell Res Ther 12: 245, 2021.
36. Zheng Q, Zhang M, Zhou F, Zhang L and Meng X: The breast cancer stem cells traits and drug resistance. Front Pharmacol 11: 599965, 2021.
37. Yoon YH, Hwang HJ, Sung HJ, Heo SH, Kim DS, Hong SH, Lee KH and Cho JY: Upregulation of complement factor H by SOCX-1/3-STAT4 in lung cancer. Cancers (Basal) 11: 471, 2019.
38. Martin M, Leffler J, Smolag KI, Mytych J, Björk A, Chaves LD, Alexander JJ, Quigg RJ and Blom AM: Factor H uptake regulates intracellular C3 activation during apoptosis and decreases the inflammatory potential of nucleosomes. Cell Death Differ 23: 903-911, 2016.
39. Mao X, Zhou L, Tey SK, Ma APY, Yeung CLS, Ng TH, Wong SWK, Liu BHM, Fung YME, Patz EF Jr, *et al*: Tumour extracellular vesicle-derived complement factor H promotes tumorigenesis and metastasis by inhibiting complement-dependent cytotoxicity of tumour cells. J Extracell Vesicels 10: e12031, 2020.
40. Gupta N, Mohan CD, Shanmugam MK, Jung YY, Chinnathambi A, Alharbi SA, Ashrafizadeh M, Mahale M, Bender A, Kumar AP, *et al*: CXCR4 expression is elevated in TNBC patient derived samples and Z-guggulsterone abrogates tumor progression by targeting CXCL12/CXCR4 siganling axis in preclinical breast cancer model. Environ Res 232: 116335, 2023.
41. Alsaab HO and Almalki AH: Anti-HSP70 alleviates cell migration and proliferation in colorectal cancer cells (CRC) by targeting CXCR4 (in vitro study). Med Oncol 40: 256, 2023.
42. Zhao H, Jiang R, Zhang C, Feng Z and Wang X: The regulatory role of cancer stem cell marker gene CXCR4 in the growth and metastasis of gastric cancer. NPJ Precis Oncol 7: 86, 2023.
43. To SQ, Dmello RS, Richards AK, Ernst M and Chand AL: STAT3 signaling in breast cancer: Multicellular actions and therapeutic potential. Cancers (Basel) 14: 429, 2022.
44. Zeng R, Liu Y, Jiang ZJ, Huang JP, Wang Y, Li XF, Xiong WB, Wu XC, Zhang JR, Wang QE and Zheng YF: EPB41L3 is a potential tumor suppressor gene and prognostic indicator in esophageal squamous cell carcinoma. Int J Oncol 52: 1443-1454, 2018.
45. Lu Y, Liu B, Liu Y, Yu X and Cheng G: Dual effects of active ERK in cancer: A potential target for enhancing radiosensitivity. Oncol Lett 20: 993-1000, 2020.
46. Sambade M, Camp JT, Kimple RJ, Sartor CI and Shields JM: Mechanism of lapatinib-mediated radiosensitization of breast cancer cells is primarily by inhibition of the Raf>MEK>ERK mitogen-activated protein kinase cascade and radiosensitization of lapatinib-resistant cells restored by direct inhibition of MEK. Radiother Oncol 93: 639-644, 2009.
47. He H, Lin K, Zou C, Pan J, Fu W, Zhou Y, Lin H, Chen C and Su Y: Knockdown of annexin A2 enhances radiosensitivity by increasing G2/M-phase arrest, apoptosis and activating the p38 MAPK-HSP27 pathway in nasopharyngeal carcinoma. Front Oncol 12: 769544, 2022.
48. Zhou Y, Zhao W, Xie G, Huang M, Hu M, Jiang X, Zeng D, Liu J, Zhou H, Chen H, *et al*: Induction of Nur77-dependent apoptotic pathway by a coumarin derivative through activation of JNK and p38 MAPK. Carcinogenesis 35: 2660-2669, 2014.
49. Tang J, Wu W, Yang F, Liu L, Yang Z, Liu L, Tang W, Sun F and Lin H: Marine sponge-derived smenospongine preferentially eliminates breast cancer stem-like cells via p38/AMPKa pathways. Cancer Med 7: 3965-3976, 2018.